Haptic-guiding to avoid collision during teleoperation

Disha Kamale* †1, Sariah Mghames* †1, Tommaso Pardi‡1, Aravinda R. Srinivasan†2, Gerhard Neumann‡2 and Amir Ghalamzan E.* †1

I. Introduction

Tele-operating a robotic manipulator, called slave-arm (SA) imposes a high cognitive load even on expert human operators and, consequently, results in severe fatigue and progressive degeneration in performance [1], [2]. An operator usually steers a SA to reach an object (reach-to-grasp - g_0), form stable contacts between SA fingers and object (grasp synthesis - g_1) and move the object (post-grasp manipulative movement - g_2). Predicting collision during autonomous post-grasp is non-intuitive and operators typically perform several grasp-move-drop sequences in order to avoid situations wherein the robot might get close to collision, e.g., this happens many times in robotic surgery [3].

In addition to easing out teleoperation, a haptic feeling proportional to forces/torques applied to robot joints may help deliver additional information about the workspace constraints such as collisions, joint limits, and singularities. In these cases, the haptic device generates Haptic Force Cues (HFC) which are proportional to the gradient of computed cost values. For instance, HFCs are used to inform the operator of instantaneous collision, singularities and joint limits in dual-arm [4] and single-arm manipulation [5] as well as along a predicted SA trajectory [6] such as g_0 motion [7], [8]. The above non-conventional use of HFCs approaches can significantly improve the teleoperation experience. However, receiving haptic-force cues, albeit extremely useful, is sometimes not intuitive and might cause additional cognitive load on the operator [7].

We assume g_0 can be efficiently performed by a human operator while g_2 movements can be autonomously performed. Previous approaches have strong limitations that affect the flexibility of the operator and can cause discomfort. We develop a new strategy for haptic-guidance to inform an operator of a grasp configuration that allows collision free post-grasp movements with improved flexibility and comfort of the operator.

II. Problem Formulation

We denote by $\mathcal{F}_c : \{O_c; x_n, y_c, z_c\}$ a local frame attached to the object centre of mass, with $\mathcal{F}_r : \{O_r; x_r, y_r, z_r\}$ an inertial reference frame, and by $\mathcal{F}_e : \{O_e; x_e, y_e, z_e\}$ a local frame attached to the slave arm end-effector(EE). Moreover, we denote by $\mathcal{F}_g : \{O_g; x_g, y_g, z_g\}$ a local frame representing a grasping pose candidate on the object shape.

The frame $\mathcal{F}_c$ can be expressed in $\mathcal{F}_r$ through the transformation matrix. ${}^{r}x_c \in \mathrm{SE}(3)$

$$ {}^{r}x_c(t) = \begin{bmatrix} \boldsymbol{R}_{3\times3}(t) & \boldsymbol{p}_{3\times1}(t) \\ \boldsymbol{0}_{1\times3} & 1 \end{bmatrix}, \tag{1} $$

* These authors contributed equally to this work.

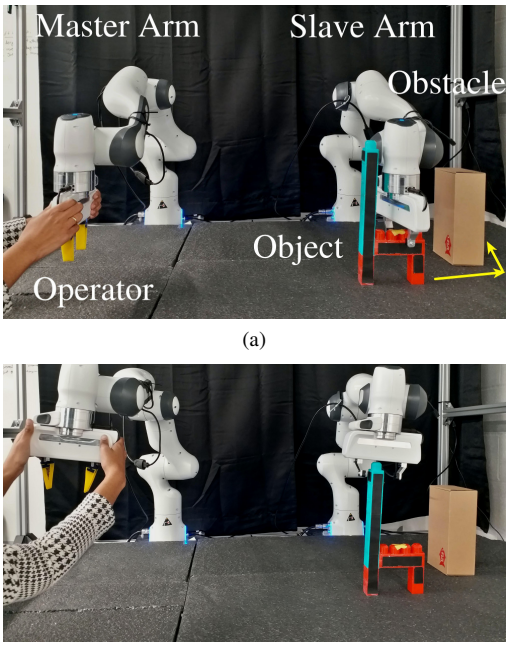

(a)

(b)

Fig. 1. Our teleoperation setup: the human operator moves the master device and the slave manipulator follows the movements of the master one.

where $\boldsymbol{p} \in \mathbb{R}^3$ and $\boldsymbol{R} \in \mathrm{SO}(3)$ are the position and orientation of any point in Cartesian space.

The trajectory to be followed by the object implies that the object frame $\mathcal{F}_c(t)$ matches a sequence of planned poses.

$$ \mathcal{F}_c(t) = \zeta(t) \qquad t \in [0, T], \tag{2} $$

where ζ is the object trajectory determining complete object poses (position and orientation) at every time $0 \leq t \leq T$ and T is the total time. Since the object is rigid and the SA EE forms stable contacts on the object surface, $\mathcal{F}_e$ becomes equal to $\mathcal{F}_g$ once stable contacts are made and $\mathcal{F}_g$ can be fully expressed at all time during post-grasp movements by a fixed transformation matrix, namely ${}^{c}x_g$, w.r.t. object local frame $\mathcal{F}_c$. The SA EE trajectory for the post-grasp movements can be computed given the planned object trajectory ζ in (2) as follows

$$ {}^{r}x_g(t) = \{{}^{r}x_c(t){}^{c}x_g : 0 \leq t \leq T\}. \tag{3} $$

Finally, the post-grasp joint configuration trajectory corresponding to a given grasping ${}^{r}x_e(t) = {}^{r}x_g(t)$, can be computed using inverse kinematics, i.e.,

$$ \hat{\boldsymbol{q}}_g(t) = \mathrm{IK}\left({}^{r}x_g(t)\right), \tag{4} $$

where $\mathrm{IK}(\cdot)$ is the slave arm inverse kinematics function which computes the joint space trajectory $\hat{\boldsymbol{q}}_g(t)$ corresponding to the grasping frame trajectory $\mathcal{F}_g(t)$. The collision cost computation is similar to [7].

A. Cost Gradient

We consider a stacked vector of the slave arm linear ($\dot{\boldsymbol{p}} \in \mathbb{R}^3$) and angular ($\boldsymbol{\omega} \in \mathbb{R}^3$) velocities during reach-to-grasp by $\dot{x}_e = [\dot{\boldsymbol{p}}^T, \boldsymbol{\omega}^T]^T$, where

$$ {}^r\dot{x}_e = {}^r\bar{\boldsymbol{R}}_c \, {}^c\dot{x}_g, \quad {}^r\bar{\boldsymbol{R}}_c = \begin{bmatrix} {}^r\boldsymbol{R}_c & \boldsymbol{O} \\ \boldsymbol{O} & {}^r\boldsymbol{R}_c \end{bmatrix} \tag{5} $$

and ${}^r\bar{\boldsymbol{R}}_c \in \mathbb{R}^{6\times6}$ transforms the twist $\dot{x}_g$ from $\mathcal{F}_c$ to $\mathcal{F}_r$. Combining the SA differential forward kinematics, *i.e.* ${}^r\dot{x}_e = \boldsymbol{J}_s(\boldsymbol{q}_s)\dot{\boldsymbol{q}}_s$ (where $\boldsymbol{J}_s$ is the conventional slave arm geometric Jacobian)[1] , and (5) yields

$$ \dot{\boldsymbol{q}}_s = \boldsymbol{J}_s^{\dagger}(\boldsymbol{q}_s) \, {}^r\bar{\boldsymbol{R}}_c \, {}^c\dot{x}_g, \tag{6} $$

where $\boldsymbol{J}_s^{\dagger}$ denotes the usual $\boldsymbol{J}_s$ Moore-Penrose pseudoinverse. Equation (6) will be exploited in the following Section to generate haptic-guidance force cues. Using Leibniz's formulas and the chain rule, we can write

$$ \nabla_{{}^c x_g}\mathcal{H} = \frac{\partial \mathcal{H}}{\partial {}^c x_g} = \int_0^{s^\star} \frac{\partial h}{\partial {}^c x_g} \mathrm{d}s, \tag{7} $$

where $s^\star$ is the arc length of the curve, and

$$ \frac{\partial h}{\partial {}^c x_g} = \frac{\partial h}{\partial \boldsymbol{q}_s} \frac{\partial \boldsymbol{q}_s}{\partial {}^c x_g}. \tag{8} $$

where the term $\partial h / \partial \boldsymbol{q}_s$ is the derivative of the cost function with respect to the generalised coordinates vector of SA. This shows the joint space direction along which the cost function increases the most. The term $\partial \boldsymbol{q}_s / \partial {}^c x_g$ can be computed from (6) as follows

$$ \frac{\partial \boldsymbol{q}_s}{\partial {}^c x_g} = \boldsymbol{J}_s^{\dagger}(\boldsymbol{q}_s) \, {}^r\bar{\boldsymbol{R}}_c, \tag{9} $$

and depends only on the robot kinematics and the transformation from the object's frame and the global inertial reference frame. Substituting in (8), it yields

$$ \frac{\partial h}{\partial {}^c x_g} = \frac{\partial h}{\partial \boldsymbol{q}_s} \boldsymbol{J}_s^{\dagger}(\boldsymbol{q}_s) \, {}^r\bar{\boldsymbol{R}}_c. \tag{10} $$

The partial derivatives of h w.r.t. $\boldsymbol{q}_s$ can be easily computed and then plugged in (10).

We consider a classical bilateral force-feedback system. We want to generate some force cues at MA which inform the operator of the cost gradient. The operator interacts with MA by applying some forces to move it. MA is coupled (via velocity-velocity mirroring) with a SA.

Let $\mathcal{F}_m$ be the base frame of the master device, here taken w.l.o.g. as parallel to the based frame $\mathcal{F}_r$ of the slave arm. Let ${}^m\mathbf{x}_M \in \mathbb{R}^6$ represent the Cartesian position and orientation of the master device in $\mathcal{F}_m$: the master device is modelled as a generic (gravity pre-compensated) mechanical system

$$ \boldsymbol{M}({}^m\mathbf{x}_M) \, {}^m\ddot{\mathbf{x}}_M + \boldsymbol{C}({}^m\mathbf{x}_M, \, {}^m\dot{\mathbf{x}}_M) \, {}^m\dot{\mathbf{x}}_M = \bar{\boldsymbol{\tau}} + \boldsymbol{\tau}_h, \tag{11} $$

where $\boldsymbol{M}({}^m\mathbf{x}_M) \in \mathbb{R}^{6\times6}$ is the the positive-definite and symmetric inertia matrix, $\boldsymbol{C}({}^m\mathbf{x}_M, \, {}^m\dot{\mathbf{x}}_M) \in \mathbb{R}^{6\times6}$ consists of Coriolis/centrifugal terms, and $\bar{\boldsymbol{\tau}}$, $\boldsymbol{\tau}_h \in \mathbb{R}^6$ are the control and human forces, respectively, applied at MA end-effector. In principal, ${}^r\dot{x}_g = \alpha \, {}^m\dot{\mathbf{x}}_M$, where ${}^r\dot{x}_g, {}^m\dot{\mathbf{x}}_M$ are the master and slave EEvelocities. MA and SA, in our example, have the same kinematics so $\alpha = 1$ (the MA/SA scaling factor).

[1]Subscript $*_e$ refers to the EE during reach-to-grasp whereas $*_g$ refers to the EE after making stable contacts between the EE and the object.

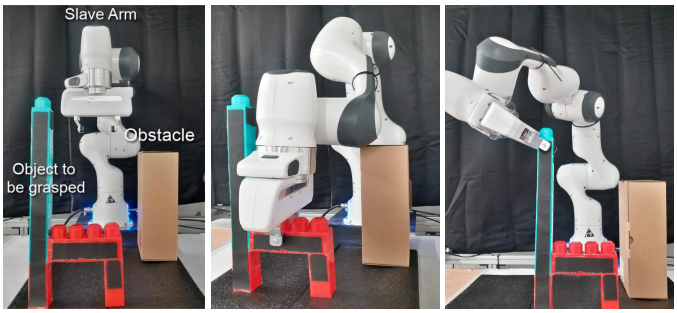

(a) Initial pose (b) Collision (c) Good grasp

Fig. 2. Snapshots of the SA workspace during experimenting Task II: 2a shows the SA, object and obstacle at the beginning of Task II experiments; 2b shows SA link next to its wrist collides with the obstacle during performing Task II by a chosen grasp on the horizontal bar of the object; 2c shows collision free movements of the SA by a good choice of grasp.

We want the haptic-feedback informs the user of gradient decent direction of the collision cost. We design force cues $\mathbf{f} \in \mathbb{R}^6$ aligned with the negative gradient given in eq. (7), i.e.,

$$ \boldsymbol{\tau} = -\mathbf{B} \, {}^m\dot{\mathbf{x}}_M - \mathbf{K}_m \mathbf{Q} \frac{\partial \mathcal{H}}{\partial {}^c x_g}^T \tag{12} $$

where $\mathbf{K}_m$ is a scaling factor and $\mathbf{Q}$ maps the quaternion rate resulting from the gradient, in eq. (7), into a corresponding angular velocity and rotates the result in the master base frame. We add a damping term to the force cues with a positive definite damping matrix $\mathbf{B} \in \mathbb{R}^{6\times6}$ to make the force feedback signal $\bar{\boldsymbol{\tau}}$ feel more stable (see [7] for more details).

References

[1] M. Talha, "Towards robotic decommissioning of legacy nuclear plant: Results of human-factors experiments with tele-robotic manipulation, and a discussion of challenges and approaches for decommissioning," in *IEEE Int. Symp. on Safety, Security, and Rescue Rob.*, 2016, pp. 166–173.

[2] L. Peternel, N. Tsagarakis, D. Caldwell, and A. Ajoudani, "Adaptation of robot physical behaviour to human fatigue in human-robot co-manipulation," in *2016 IEEE-RAS 16th International Conference on Humanoid Robots (Humanoids)*, Nov 2016, pp. 489–494.

[3] G. A. F. et al., "A new laparoscopic tool with in-hand rolling capabilities for needle reorientation," *IEEE Rob. Autom. Lett.*, vol. 3, no. 3, pp. 2354–2361, 2018.

[4] M. e. a. Selvaggio, "Haptic-based shared-control methods for a dual-arm system," *IEEE Robotics and Automation Letters*, vol. 3, no. 4, pp. 4249–4256, 2018.

[5] F. e. a. Abi-Farraj, "A visual-based shared control architecture for remote telemanipulation," in *IEEE/RSJ International Conference on Intelligent Robots and Systems (IROS)*. IEEE, 2016, pp. 4266–4273.

[6] N. e. a. Pedemonte, "Visual-based shared control for remote telemanipulation with integral haptic feedback," in *2017 IEEE International Conference on Robotics and Automation (ICRA)*. IEEE, 2017, pp. 5342–5349.

[7] A. Ghalamzan E. , F. Abi-Farraj, P. R. Giordano, and R. Stolkin, "Human-in-the-loop optimisation: Mixed initiative grasping for optimally facilitating post-grasp manipulative actions," in *IEEE/RSJ Int. Conf. Intell. Rob. Syst.*, 2017, pp. 3386–3393.

[8] M. e. a. Selvaggio, "Haptic-guided shared control for needle grasping optimization in minimally invasive robotic surgery," in *IEEE/RSJ International Conference Intelligent Robotic System*, 2019.